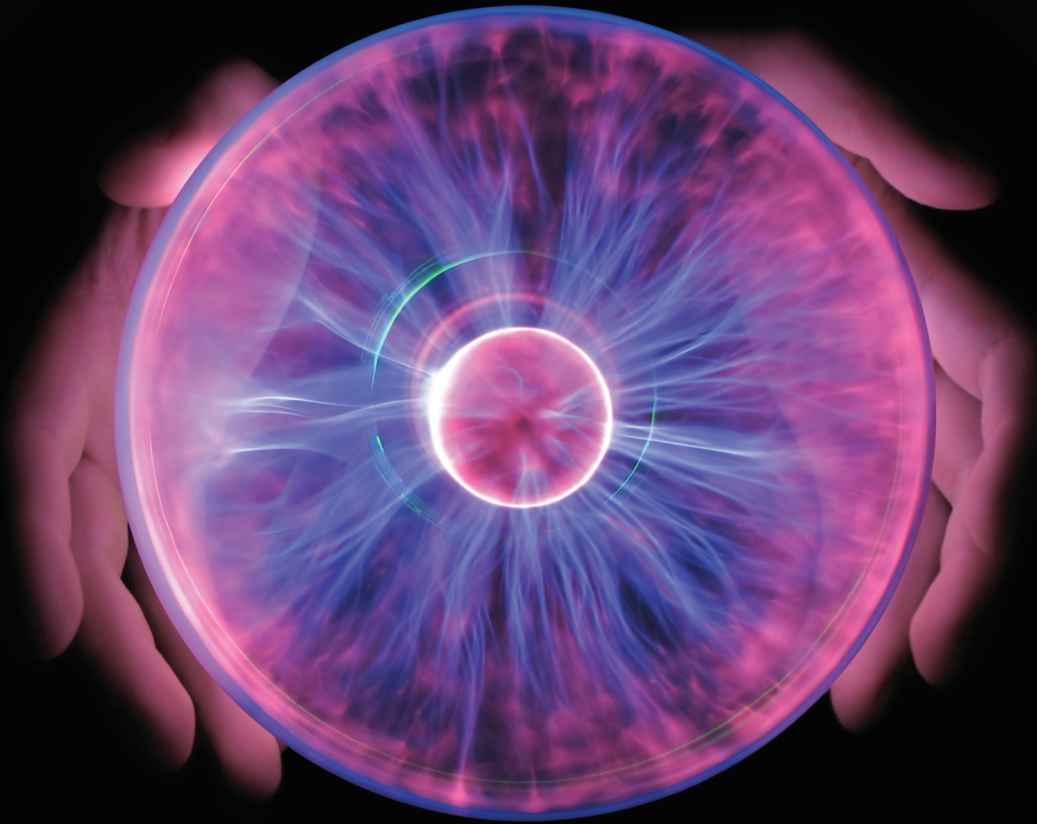


Gadobrix[®] 1.0

7mL/PFS

9.5mL/PFS

| Gadobutrol |



Optimal dosage for diagnosis

- 1.0mmol/mL high concentration
- High Stability of Macrocyclic compound
- Approved for all ages
- High T1- shortening
- Whole body imaging



제조사 **TAEJOON** 태준제약



판매자



Pursues the Zenith of Accuracy in Medical Diagnostics

ACCUZEN



Dosimetric Effects of Air Pocket during Magnetic Resonance-Guided Adaptive Radiation Therapy for Pancreatic Cancer

Hyeonmin Jin^{1,2}, Dong-Yun Kim¹, Jong Min Park^{1,2,3,4}, Hyun-Cheol Kang¹, Eui Kyu Chie¹,
Hyun Joon An^{1,2}

¹Department of Radiation Oncology, Seoul National University Hospital, ²Biomedical Research Institute, Seoul National University Hospital,

³Institute of Radiation Medicine, Seoul National University Medical Research Center, Seoul, ⁴Robotics Research Laboratory for Extreme Environments, Advanced Institutes of Convergence Technology, Suwon, Korea

Received 8 December 2019

Revised 18 December 2019

Accepted 19 December 2019

Corresponding author

Hyun Joon An

(hjooon.an@gmail.com)

Tel: 82-2-2072-4157

Fax: 82-2-765-3317

Purpose: Online magnetic resonance-guided adaptive radiotherapy (MRgART), an emerging technique, is used to address the change in anatomical structures, such as treatment target region, during the treatment period. However, the electron density map used for dose calculation differs from that for daily treatment, owing to the variation in organ location and, notably, air pockets. In this study, we evaluate the dosimetric effect of electron density override on air pockets during online ART for pancreatic cancer cases.

Methods: Five pancreatic cancer patients, who were treated with MRgART at the Seoul National University Hospital, were enrolled in the study. Intensity modulated radiation therapy plans were generated for each patient with 60Co beams on a ViewrayTM system, with a 45 Gy prescription dose for stereotactic body radiation therapy. During the treatment, the electron density map was modified based on the daily MR image. We recalculated the dose distribution on the plan, and the dosimetric parameters were obtained from the dose volume histograms of the planning target volume (PTV) and organs at risk.

Results: The average dose difference in the PTV was 0.86Gy, and the observed difference at the maximum dose was up to 2.07 Gy. The variation in air pockets during treatment resulted in an under- or overdose in the PTV.

Conclusions: We recommend the re-contouring of the air pockets to deliver an accurate radiation dose to the target in MRgART, even though it is a time-consuming method.

Keywords: MR-guided radiotherapy, Adaptive radiotherapy, Interfractional motion, Pancreatic neoplasm, Air pocket

Introduction

Pancreatic cancer is one of the most aggressive tumors, with a reported five-year overall survival range within 5%–20%. For a patient with locally advanced pancreatic cancer (LAPC), which is an unresectable disease, treat-

ment usually consists of chemotherapy or a combination of chemotherapy and radiation therapy.^{1,2)} Stereotactic body radiation therapy (SBRT), used for precise targeting and dose escalation, has demonstrated an improved local control rate in LAPC. However, SBRT for LAPC presents several challenges, despite its impressive local control rate;

increased gastrointestinal toxicity²⁾ and the delineation of pancreatic tumors and their surrounding organs remain as issues.

The advent of magnetic resonance-guided radiation therapy (MRgRT) addressed these problems. Compared to conventional computed tomography (CT) or cone-beam CT imaging, the MR image offered superior soft tissue contrast. During treatment, real-time soft tissue imaging from MR can be used to localize the target and the tumor motion can be tracked. This is advantageous in abdominal disease sites, especially when using the SBRT technique. It enables the delivery of hypo-fractionated radiotherapy with tight margins.

More recently, online MR-guided adaptive radiotherapy (MRgART) has been proposed to address the changes in anatomical structures, such as the treatment target region, during the treatment period.^{3,4)} In the MRgART workflow, the structures are re-contoured at each fraction, while the patient is on the couch, and the plan optimization and dose calculation are adapted with regard to these re-contoured anatomical variations. This technique can take into account both intra-fraction respiratory motion and inter-fraction physiologic organ variations, allowing the accurate administering of higher doses while avoiding damage to critical structures.⁴⁾

Despite these advantages, physical limitations still remain in the dose calculation for MRgART. The electron

density is an essential factor for accurate dose calculation. However, the MR signals are related to the proton density and relaxation properties of tissue, not to electron density. The common strategy, as shown in Fig. 1, consists of applying rigid or deformable registration, from CT to MRI, and assigning an electron density map obtained from the registered CT. An important point to consider is that the presence of air pockets in the organs can affect dose calculation based on registration between MR and CT images. Regardless of how accurate the registration algorithm is, it cannot take into account the irregular movements of the air pockets. Air pocket variability in the bowel and stomach is commonly observed in clinical practice in MR imaging. Several studies have reported that air pockets influence the calculation of the dose distribution in the vaginal and pancreatic regions.⁵⁻⁷⁾

In this study, we retrospectively compared the dosimetric effects of overriding the electron density map on the air pockets in online adaptive radiotherapy for pancreatic cancer.

Materials and Methods

1. Patient selection and planning

Five pancreatic cancer patients, who received MRgRT at Seoul National University Hospital, were retrospectively

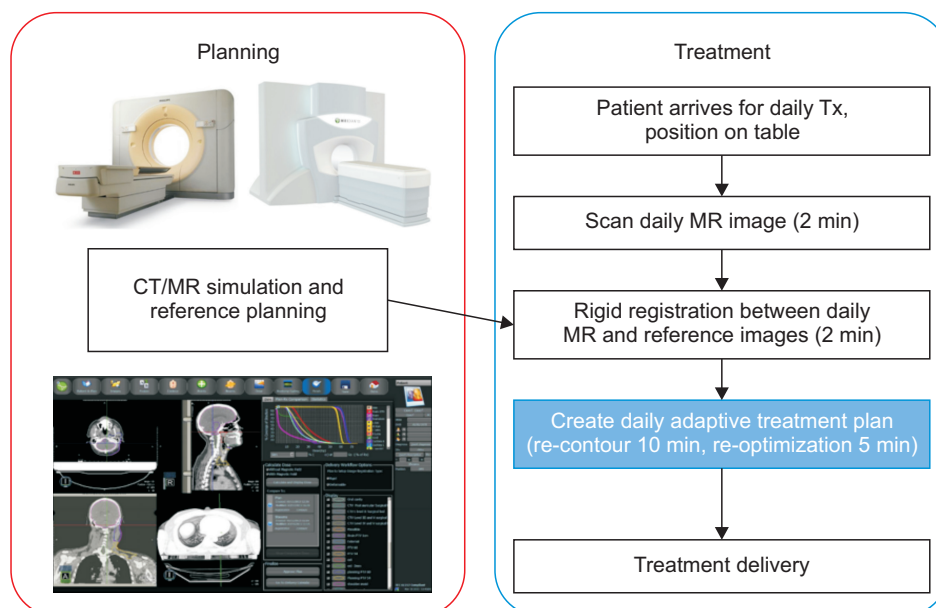


Fig. 1. Workflow of the magnetic resonance (MR)-guided online adaptive radiotherapy. CT, computed tomography.

enrolled in the study. During the CT simulation process, each patient was properly immobilized with MR dummy coils, which is similar to the setup for MR simulation and treatment. The simulated CT images were acquired with the Brilliance CT Big Bore™ (Philips, Amsterdam, Netherlands) system, and the simulated MR images were scanned with the ViewRay® system, using an identical setup and the same immobilization devices.

For pancreatic cancer treatment with MRgRT, a prescription dose of 45 Gy, with a daily dose of 9 Gy, was planned to the planning target volume. A single oncologist defined the target volume and the organs at risk (OARs) for this study. Some organs such as the spinal cord, kidney, bowel, stomach, and duodenum were selected as OARs, according to the tumor location.

The optimization and dose calculation were performed using the MRIdian system. The dose distributions were computed using the Monte Carlo algorithm, developed by the manufacturer, with a 0.35 T magnetic field condition. The grid size of the dose calculation was set to 3 mm. If the dose incident on the OARs exceeded the tolerance level, we changed the optimization parameters and the optimization process was repeated, until the tolerance level was met. Every plan was normalized to cover 95% of the planning target volume (PTV) with 100% of the prescription dose.

2. Electron density modification

Patients received daily MR images before treatment for isocenter localization matching. For each fraction, the images were fused to the simulation MR using rigid registration, as shown in Fig. 1. When the locations significantly changed, the OAR and air pockets were contoured. We also identified the body contour using the automatic segmentation function on the treatment planning system.

We modified the electron density map, overridden with air or water electron density, depending on the variation of cavities in the MR images. When the air pockets were localized on the planning CT, the electron density map was virtually filled with water electron density; for the daily MR image, we assigned air electron density. Furthermore, when the body contour of the planning MR was within that of the daily MR, we modified the electron density map with water density to fill the gap. For each patient, the dose was recalculated to evaluate the dosimetric effect when the electron density map was modified, owing to the variation of air pockets. The illustration of the modification of the electron density map, in terms of the air region and body contour variation in the daily MR images, is presented in Fig. 2.

3. Evaluation of treatment plans

To assess the impact of air pocket and body contour

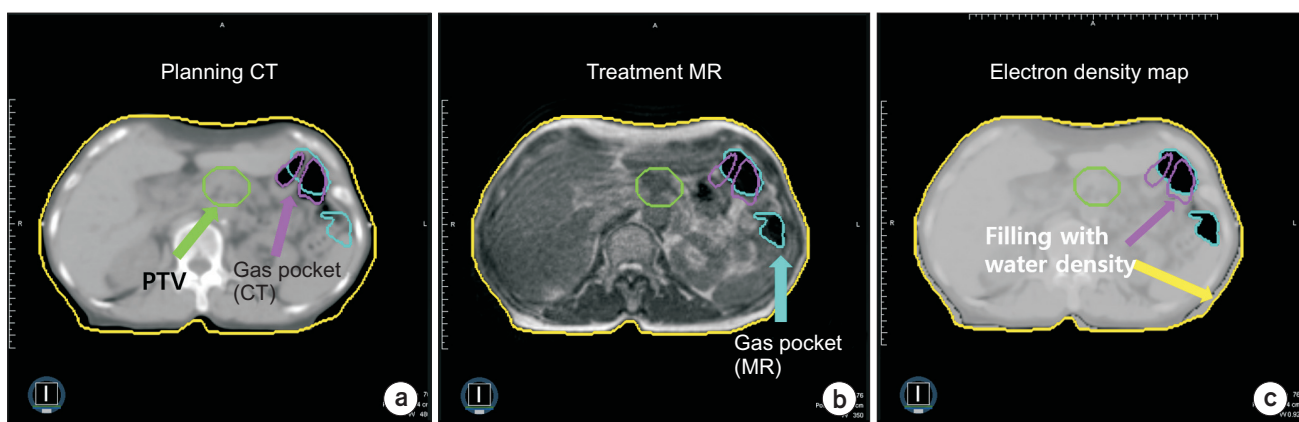


Fig. 2. Example of a modified electron density map. (a) The original planning computed tomography (CT) with the air pockets are indicated in purple. (b) Daily treatment magnetic resonance (MR) images were re-contoured at air pockets and the body, shown in blue and yellow, respectively. (c) The electron density, modified according to the variation of the air pockets and body outline. PTV, planning target volume

variation on the planning and treatment, we compared the dose-volumetric parameters of each plan, before and after the electron density override. The following doses were calculated: Near-maximum ($D_{2\%}$), near-minimum ($D_{98\%}$), $D_{90\%}$, $D_{80\%}$, $D_{5\%}$, minimum, maximum, and mean.

Dose volume histograms (DVHs) were calculated for the OARs and clinically relevant dose-volumetric parameters were measured. Statistical analysis of the dosimetric parameters was performed, using paired t-tests, with the IBM SPSS Statistics v25 software (IBM Corp., Armonk, NY, USA). A P -value less than 0.05 was considered statistically significant.

We performed 2D gamma analysis to demonstrate a map

indicating the location of the points with a large dose difference using the software 3d slicer (<http://www.slicer.org>) with radiotherapy module. The gamma criterion of 1%/1 mm was used. The study was approved by the Institutional Review Board of the Seoul National University Hospital (No. 1708-051-876).

Results

We visually evaluated the image deformation and electron density modification. Fig. 2 represents the capability of the image registration between the planning CT and the daily MR obtained during treatment. The body contour

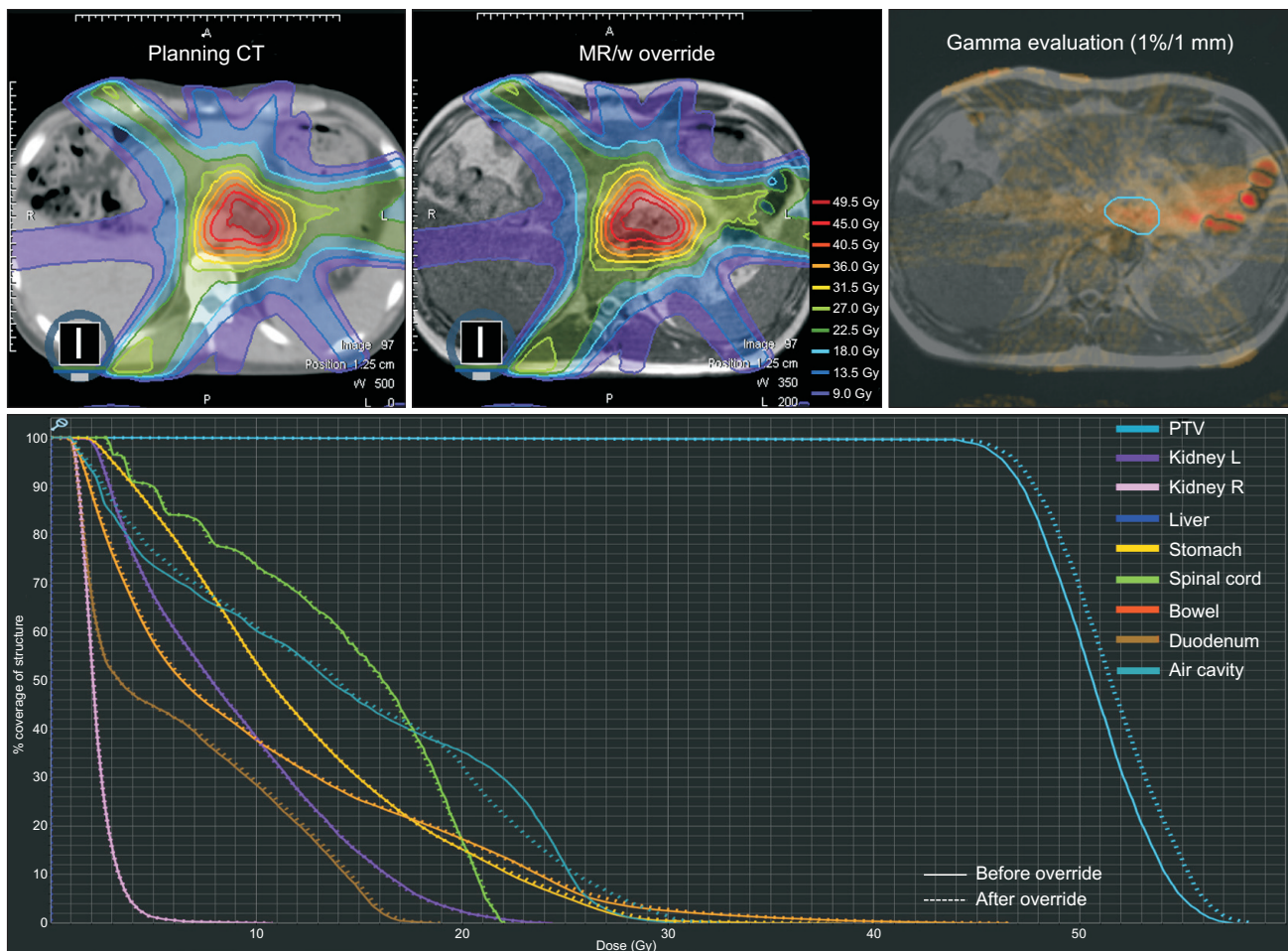


Fig. 3. A pancreas magnetic resonance image-guided radiation therapy (MRgRT) example, with air pockets located near the planning target volume (PTV) and on the beam path. The calculated dose distribution before overriding the air pockets on planning computed tomography (CT) (top left), after overriding those on treatment MR (top middle), and the gamma map between two dose distributions (top right) are represented. Dose volume histograms (DVHs) of the PTV, kidney, liver, stomach, spinal cord, bowel, duodenum, and air pocket of MR are shown at the bottom. The dashed and solid lines represent the DVHs calculated from the plans before and after the electron density map override, respectively.

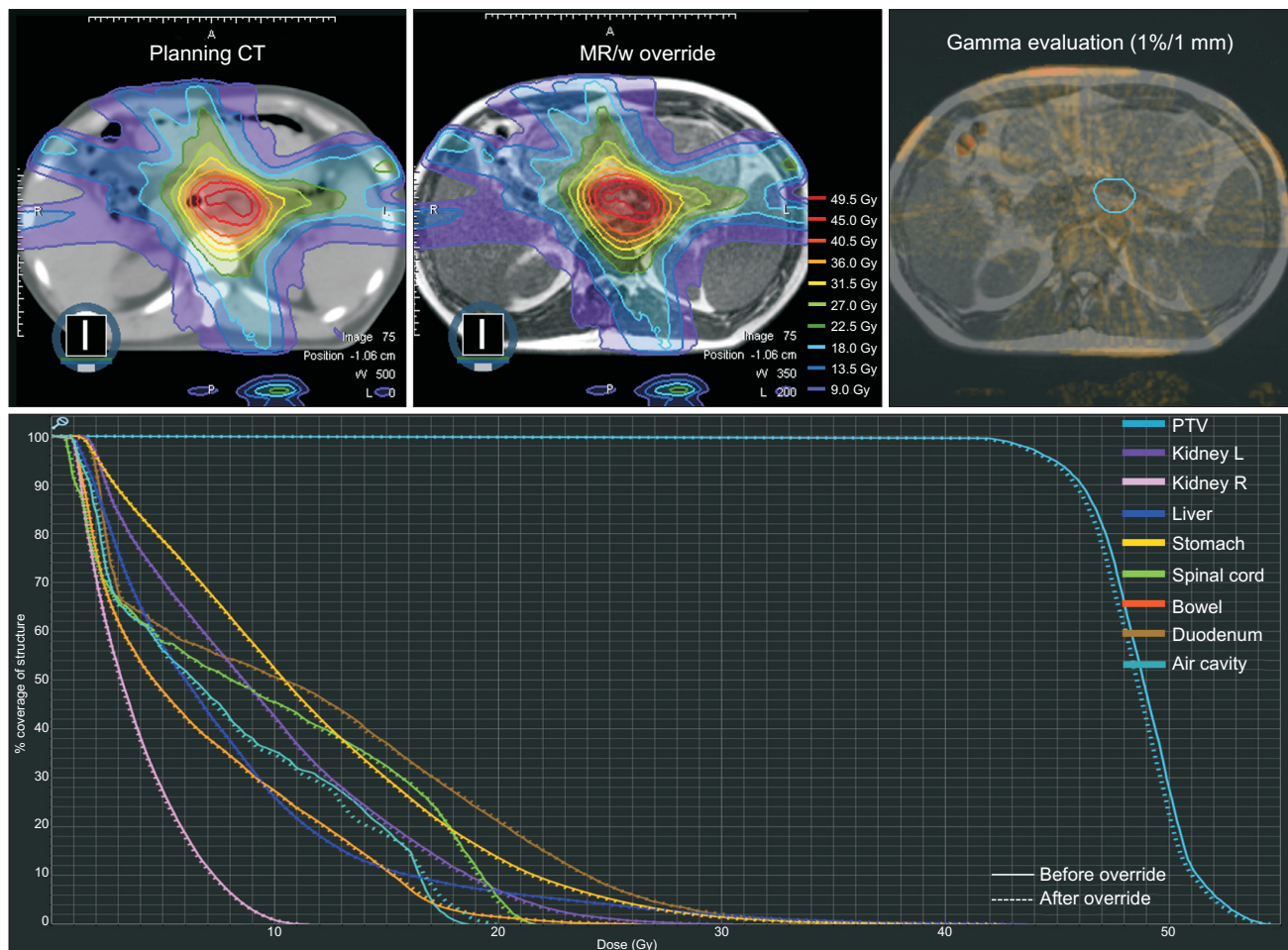


Fig. 4. A pancreas magnetic resonance image-guided radiation therapy (MRgRT) example, with air pockets located relatively far from the planning target volume (PTV). The calculated dose distribution before overriding the air pockets on planning computed tomography (CT) (top left), after overriding those on treatment MR (top middle), and the gamma map between two dose distributions (top right) are represented. Dose volume histograms (DVHs) of the PTV, kidney, liver, stomach, spinal cord, bowel, duodenum, and air pocket of MR are shown at the bottom. The dashed and solid lines represent the DVHs calculated from the plans before and after the electron density map override, respectively.

delineated in the treatment images showed some disagreement with the planning CT at the edges. The locations of air pockets were also different between the planning CT and the daily MR images. The modified electron density map, filled with water density according to the variation of the air pockets and body outline, is shown in Fig. 2c.

We selected a sample case for which the air pockets, located near the PTV, were on the beam path, shown in Fig. 3. The air pockets in the MR were overridden with water density and the plan was recalculated, as shown in Fig. 3b. The gamma map, computed to represent the dose differences between the two plans, was overlaid with the MR image to determine the air pocket location. The gamma values were

higher in the air pocket regions on the left side of the target volume, compared to other areas. The predicted dose on the target volume also varied, due to the electron density override. The cumulative DVHs for this patient show a discrepancy, especially in the slope of PTV.

Another sample case for the air pockets, located relatively far from the PTV, is represented in Fig. 4. Small air pockets were scattered in the abdomen, and their positions were similar between the planned CT and daily treatment scan images. Only the contours of the body showed a difference in the dose distribution. In this case, there were no noticeable changes in the DVHs.

We evaluated the overall effect of the variation of the air

Table 1. Dosimetric parameter analysis for the target volume

Dose-volumetric parameter	Before modification	After modification	Absolute difference	P-value
PTV volume (cm ³)	35.5 (26.7–60.6)			
D _{98%} (Gy)	43.5 (40.4–45.5)	43.2 (38.8–46.0)	0.71 (0.20–1.67)	0.47
D _{95%} (Gy)	45.1 (44.0–46.6)	44.8 (42.0–47.3)	0.78 (0.23–1.93)	0.49
D _{5%} (Gy)	53.0 (48.3–60.4)	52.7 (47.7–58.2)	0.94 (0.25–2.26)	0.65
D _{2%} (Gy)	53.7 (48.5–61.6)	53.4 (48.0–59.3)	0.93 (0.28–2.32)	0.6
Minimum dose (Gy)	38.7 (31.3–42.0)	38.5 (30.3–42.0)	0.47 (0.17–1.07)	0.57
Maximum dose (Gy)	54.9 (49.3–63.6)	54.6 (48.7–60.9)	1.00 (0.13–2.74)	0.64
Mean dose (Gy)	49.3 (46.8–52.7)	49.0 (46.3–51.8)	0.86 (0.27–2.07)	0.61

Table 2. Dosimetric parameter analysis for the organs at risks

Dose-volumetric parameter	Before modification	After modification	Absolute difference	P-value
Spinal Cord Dmax (Gy)	17.9 (11.9–22.0)	17.8 (12.1–21.9)	0.25 (0.06–0.63)	0.63
Duodenum D _{0.5cc} (Gy)	21.3 (14.9–28.3)	21.3 (15.1–27.6)	0.33 (0.07–0.67)	0.82
Duodenum D _{10cc} (Gy)	16.3 (8.5–24.6)	16.2 (8.5–24.1)	0.22 (0.03–0.47)	0.35
Stomach D _{0.5cc} (Gy)	31.3 (26.0–39.7)	31.0 (25.7–39.7)	0.54 (0.06–1.56)	0.48
Stomach D _{10cc} (Gy)	27.9 (24.5–31.1)	27.6 (24.2–31.1)	0.46 (0.03–1.26)	0.47
Bowel D _{0.5cc} (Gy)	25.5 (18.0–35.6)	25.6 (18.2–36.0)	0.52 (0.08–1.19)	0.90
Bowel D _{10cc} (Gy)	22.8 (15.5–33.0)	22.8 (15.6–32.5)	0.49 (0.04–1.09)	0.87

pockets on MRgRT. Table 1 presents the results of the average dosimetric parameters for the target volume. The dose volumetric parameters in the PTV were calculated on two plans—with or without the overriding of electron density on air pockets in the MR. The average absolute difference in the mean dose was 0.86 Gy and the maximum difference was 2.07 Gy. The average absolute differences in Dmin and Dmax were 0.47 Gy and 1.00 Gy, respectively. The averages of D_{2%} were 53.73 Gy and 53.41 Gy, before and after electron density modification, respectively. However, the absolute difference in D_{2%} was up to 2.32 Gy. For all dosimetric parameters of the PTV, there were no statistically significant differences.

For the spinal cord, the average Dmax was 17.9 Gy and 17.8 Gy, before and after modification of the electron density map, respectively. The mean values of the maximum dose delivered to a volume of 0.5 cc in the duodenum were 21.3 Gy for both plans. For the stomach, the absolute difference in D_{0.5cc} was up to 1.6 Gy, in our dataset. There were also no statistically significant differences in the dosimetric parameters of OARs. Other dosimetric parameters for the OARs are summarized in Table 2.

Discussion

The advantage of using the MRgART is the reduction in uncertainty. This is achieved through managing the interfraction organ location variability by scanning the MR before treatment.^{3,8,9)} Additional to identifying the organ location, determining the electron density map for dose calculation is also of importance. The MR-based adaptive treatment planning procedure computes the dose distribution based on the planning CT images. In particular, the different locations of the air pockets, which have lower Hounsfield Units compared to that of soft tissue, affect the dose calculation.¹⁰⁾ Therefore, we retrospectively evaluated the dosimetric effects on the modified electron density map, which was overridden with water density, according to the MR images during daily treatment for pancreas SBRT.

Despite the lack of statistically significant differences between the cases with and without the density override plans, the air pockets may be relevant to the dose distribution on the PTV. Specifically, the absolute difference of D95% between the two plans was up to 1.93 Gy for patient 2, owing to the electron density override effect. The pho-

ton transmission was affected when the air pockets were located within the beam path,¹¹⁾ but the effectiveness was dependent on the volume of gastrointestinal gas and location changes. It is difficult to predict the dose distribution in the target volume that would be considered an under- or overdose, compared to the original plan, because beams of different angles must be considered for such a prediction. Therefore, we instructed the patient on dietary specifications to reduce the variability of gastrointestinal organ volumes and to minimize the gas formed in clinical practice. Despite these efforts, the stomach and bowel gas variability are an inevitable issue in radiotherapy.

Adaptive radiotherapy is one of the solutions for the management of organ motions, including bowel gas patterns. In particular, re-planning with the daily MR image gives an advantage of improved soft-tissue contrast resolution, compared to traditional X-ray. However, a major obstacle when using ART is the extensive workload required for editing the re-contouring and re-optimization. Our study showed that the $D_{95\%}$ of PTV had an average difference of 1.08% (maximum 4.29%) to the prescription dose, when the electron density map was not modified in the air pocket. Bohoudi et al.¹²⁾ suggested the limited re-contouring strategy for plan adaptation, applicable only to the OARs within 3 cm of the PTV. This strategy can be applied to reduce time-consuming work, but assessing its effects on dosimetric parameters is beyond the scope of this study.

Recently, automatic segmentation algorithms, related to deep learning, were studied to reduce the delineation work of OARs and the target volume.¹³⁾ It is possible to apply these algorithms in the clinical workflow, in terms of the computational time, because approximately a few seconds are required for the segmentation of OARs. Furthermore, syntactic CT generation has been proposed for MR-only radiotherapy, which is directly converted from MRI scans.^{13,14)} The primary advantage of this technique is its ability to minimize the variation in organ location, especially the unpredictable air pocket, between the time of simulation and treatment. These recent image processing techniques have the potential to reduce the time-consuming work and uncertainty of the dose delivery in ART.

Our study has several limitations. The sample size may have been too small to show a statistically significant dif-

ference between the two dose distributions. Another limitation of the study is the assessment of the electron density override effect by combining two variations of air pockets and body outline. The impact of the interfraction variation of the body contour is relatively small, owing to the distance from the target volume in pancreatic cancer. However, it is necessary to comprehensively analyze each of the two effects in future studies.

Conclusions

The variation in air pockets in a patient's gastrointestinal area causes a difference between the electron density map used for dose calculation and those used for daily treatment. These differences may result in an under- or overdose in the PTV. The recalculation of a patient's dose, based on the modified electron density map, reduced the uncertainties related to the dose. Therefore, when air pockets are located near the target volume, we recommend performing the delineation of the air pocket to deliver an accurate radiation dose to the target, even though this method is time-consuming.

Acknowledgements

This study was supported by a grant from the National Research Foundation of Korea (NRF) grant funded by the Korean government (MSIP) (No. 2019M2A2B4095126).

Conflicts of Interest

The authors have nothing to disclose.

Availability of Data and Materials

All relevant data are within the paper and its Supporting Information files.

Ethics Approval and Consent to Participate

The study was approved by the institutional review board (IRB approval number; No.1708-051-876).

References

1. Hidalgo M. Pancreatic cancer. *N Engl J Med*. 2010;362:1605-1617
2. Wang F, Kumar P. The role of radiotherapy in management of pancreatic cancer. *J Gastrointest Oncol*. 2011;2:157-167.
3. Boldrini L, Cusumano D, Cellini F, Azario L, Mattiucci GC, Valentini V. Online adaptive magnetic resonance guided radiotherapy for pancreatic cancer: state of the art, pearls and pitfalls. *Radiat Oncol*. 2019;14:71.
4. Rudra S, Jiang N, Rosenberg SA, Olsen JR, Roach MC, Wan L, et al. Using adaptive magnetic resonance image-guided radiation therapy for treatment of inoperable pancreatic cancer. *Cancer Med*. 2019;8:2123-2132.
5. Berger T, Petersen JBB, Lindegaard JC, Fokdal LU, Tandrup K. Impact of bowel gas and body outline variations on total accumulated dose with intensity-modulated proton therapy in locally advanced cervical cancer patients. *Acta Oncol*. 2017;56:1472-1478.
6. Estabrook NC, Corn JB, Ewing MM, Cardenes HR, Das IJ. Dosimetric impact of gastrointestinal air column in radiation treatment of pancreatic cancer. *Br J Radiol*. 2018;91:20170512.
7. Onal C, Guler OC, Dolek Y. The impact of air pockets around the vaginal cylinder on vaginal vault brachytherapy. *Br J Radiol*. 2015;88:20140694.
8. Hunt A, Hansen VN, Oelfke U, Nill S, Hafeez S. Adaptive radiotherapy enabled by MRI guidance. *Clin Oncol (R Coll Radiol)*. 2018;30:711-719.
9. Keall P, Poulsen P, Booth JT. See, think, and act: real-time adaptive radiotherapy. *Semin Radiat Oncol*. 2019;29:228-235.
10. Klein EE, Chin LM, Rice RK, Mijnheer BJ. The influence of air cavities on interface doses for photon beams. *Int J Radiat Oncol Biol Phys*. 1993;27:419-427.
11. Paudel MR, Kim A, Sarfehnia A, Ahmad SB, Beachey DJ, Sahgal A, et al. Experimental evaluation of a GPU-based Monte Carlo dose calculation algorithm in the Monaco treatment planning system. *J Appl Clin Med Phys*. 2016;17:230-241.
12. Bohoudi O, Bruynzeel AME, Senan S, Cuijpers JP, Slotman BJ, Lagerwaard FJ, et al. Fast and robust online adaptive planning in stereotactic MR-guided adaptive radiation therapy (SMART) for pancreatic cancer. *Radiother Oncol*. 2017;125:439-444.
13. Spieler B, Patel NV, Breto AL, Ford J, Stoyanova R, Zavala-Romero O, et al. Automatic segmentation of abdominal anatomy by artificial intelligence (AI) in adaptive radiotherapy of pancreatic cancer. *Int J Radiat Oncol Biol Phys*. 2019;105:E130-E131.
14. Men K, Zhang T, Chen X, Chen B, Tang Y, Wang S, et al. Fully automatic and robust segmentation of the clinical target volume for radiotherapy of breast cancer using big data and deep learning. *Phys Med*. 2018;50:13-19.